4-Disk Resonances

Sune Fallgaard Nielsen

January 20, 1997

1 Introduction

This report calculates the resonances of the 4-disk pinball using cycle expansion, and is an exam project given in the course: *Geometrical methods in chaos* by Predrag Cvitanović & Ronnie Mainieri at the Niels Bohr Institute, fall 1996.

A physicists quantum pinball machine is a 2-d hamiltonian scattering problem: The scattering of light waves in a plane with totally reflective circular disks ([Cv96] p.21). The resonances of the 4-disk pinball is analyzed by cycle expansion of the Gutzwiller Semi-Classical Zeta function & the computed resonances will be compared with the resonances obtained by quantum mechanics. Finally the convergence of the Gutzwiller Semi-Classical Zeta function will be demonstrated and compared with that of the dynamical zeta function.

2 4-Disk Pinball Dynamics

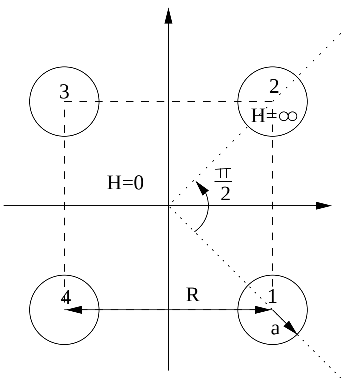

Figure 1: 4-Disk pinball system

The 4-disk pinball (figure 1) consists of 4 identical circular disks labelled:1,2,3 & 4 with radius a, each placed on the vertices of a square with a disk center to disk center distance R. The corresponding hamiltonian is ∞ within and on a disk (the disk is super reflective) and 0 elsewhere. As the four disks are equidistantly spaced, the 4-disk system has C_{4v} symmetry (see figure 3). The dynamics in the 4-disk pinball is completly described by its symbolic dynamics.

2.1 Reduced Symbolic Dynamics

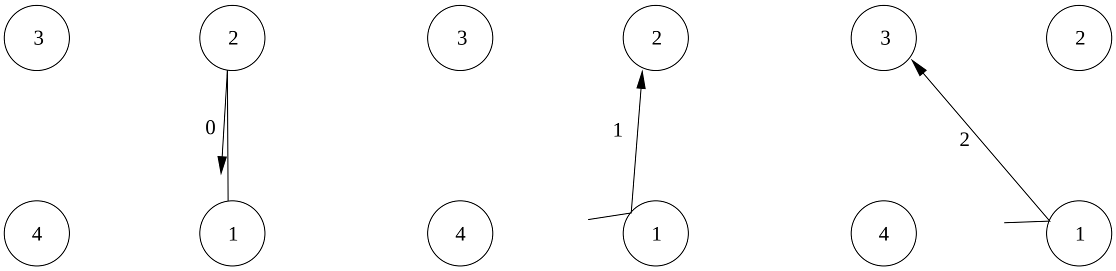

Figure 2: Illustration of the {0,1,2} symbolic dynamics on the 4-disk.

In C_{4v} the reduced symbolic dynamics are itineraries consisting of the elements: $p_i \in \{0, 1, 2\}$ (figure 2) with p_i:

0 : Rotate 1 disk position in the current orientation and flip the orientation:
clockwise rotation $\leftrightarrow$ anticlockwise rotation.

1,2 : Rotate p_i disk positions in the current orientation.

A periodic cycle p of length n is an infinite itinerary with an infinite recurrence of identical subsequences denoted: $p = \overline{p_1 p_2 \ldots p_n}$. A periodic cycle can be found to arbitrary precision (other properties ([Cv96] p.32))

$$itinerary \leftrightarrow cycle \tag{1}$$

where the dynamics takes place in the fundamental domain (figure 3), which is the C_{4v} reduction

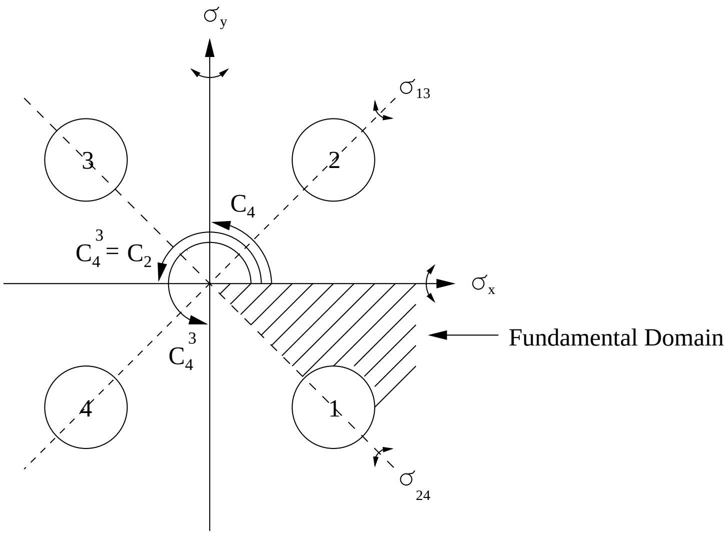

Figure 3: 4-disk geometrical group elements & the fundamental domain : An one 8'th slice of the full domain. Using the group elements the dynamics maps into the fundamental domain.

of the full domain. (C_{4v} reduced dynamics properties ([Cv96] p.291)).

When the center to center distance R is large enough the reduced symbolic dynamics is complete and pruning free (as compared to the fulldomain symbolic dynamics, figure 4)([Cv96] p.33). The calculations are done with R=6:a, a=1.

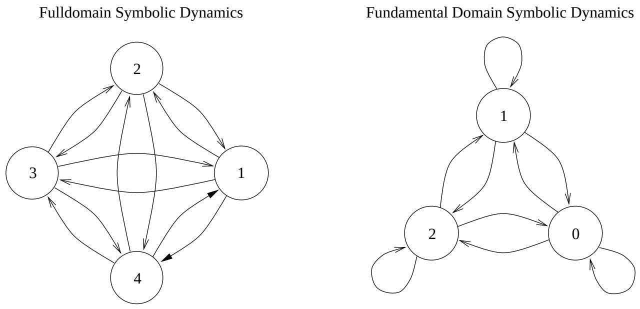

Figure 4: Markov graphs of the full domain symbolic dynamics and the reduced symbolic dynamics. The pruning of _11_, _22_, _33_, _44_ sequences in the full domain is illustrated by the absence of the self orbits.

3 Gutzwiller Semi-Classical Quantum Mechanics

The resonances or equvalently the eigenvalues of the 4-disk quantum mechanical scattering problem are the zeros of the quantum determinant (30)), section 8.

$$0 = \det\left(\widehat{H} - E(k)\right) \approx (prefactor) \cdot Z_{qm}(k) \tag{2}$$

which are approximated by the zeros of the Gutzwiller Semi-Classical Zeta function ([Wi] p.5 & [Cv96] p.319) giving the spectrum of wave numbers: $\mathcal{K} = \{k \in Z_{qm}(k) = 0\}$.

3.1 Gutzwiller trace formula

The Gutzwiller Semi-Classical Zeta function is the associated fredholm determinant of the Gutzwiller Semi-Classical Trace formula (the eigenvalues are here located at the poles $tr \to \infty$)

$$trG(E) = \overline{g}(E) + \frac{1}{i\hbar} \sum_p T_p \sum_{r=1}^{\infty} \frac{e^{-\frac{i}{\hbar} S_p(E) r + i\pi \frac{m_p}{2} r}}{\left|\det(\underline{\underline{1}} - \underline{\underline{J}}_p^r)\right|^{\frac{1}{2}}} \tag{3}$$

where the summation is done over prime orbits ([Cv96] p.318). A constant shift by the weyl term $\overline{g}(E)$ & a scaling by $\frac{1}{i\hbar}$ does not change the location of the poles and the weyl term is therefore neglected in further calculation. In the 4-disk scattering problem H(q)=0 for all periodic orbits and therefore the action integral is given by $S_p(E) = \int p dq = L_p k \hbar$, where L_p is the length of the periodic orbit p. T_p is the cycle length. Computing the maslov index m_p reduces in the scattering problem to a factor of 2 $\times$ the symbol length of the orbit (=number of disk bounces). $\underline{\underline{J}}_p$ is the linearised stability matrix along the periodic orbit. In 2-d the trace reduces to:

$$trG(k) \approx \sum_p T_p \sum_{r=1}^{\infty} \frac{e^{-\frac{i}{\hbar}L_p k\hbar r + i\pi\frac{m_p}{2}r}}{\left|\Lambda_p^r\right|^{\frac{1}{2}}\left(1-\frac{1}{\Lambda_p^r}\right)}$$

where Λ_p is the stability of the p'th orbit.

3.2 Gutzwiller Semi-Classical Zeta function

The Gutzwiller Semi-Classical Zeta function in 2-d is:

$$Z_{qm}(k) = \exp\left(-\sum_p \sum_{r=1}^{\infty} \frac{1}{r} \frac{t_p^r}{1-\frac{1}{\Lambda_p^r}}\right), t_p = \frac{e^{-\frac{i}{\hbar}L_p k\hbar + i\pi\frac{m_p}{2}}}{\left|\Lambda_p\right|^{\frac{1}{2}}} \tag{4}$$

or in product representation:

$$Z_{qm}(k) = \prod_p \prod_{k=1}^{\infty}\left(1-\frac{t_p}{\Lambda_p^k}\right) \tag{5}$$

where the multiplication is done over prime orbits. ([Cv96] p.318)

4-disk primes: 0,1,2,10,20,21,100,.... (for the number of primeorbits up to topological length n_p, look ([Cv96] p.63).)

3.3 Dynamical zeta function

The Gutzwiller Semi-Classical Zeta function relates to the dynamical zeta function $\zeta^{-1}(k)$ by

$$Z_{qm}(k) = \prod_r^{\infty} \zeta_r^{-1}(k) \tag{6}$$

with the r'th dynamical zeta function expressed as the product:

$$\zeta_r^{-1}(k) = \prod_p (1-\frac{t_p}{\Lambda_p^r}),\ t_p = \frac{e^{-i(L_p k - \pi\frac{m_p}{2})}}{|\Lambda_p|^{\frac{1}{2}}} \tag{7}$$

over prime orbits p. The dynamical zeta function is defined as $\zeta^{-1}(k) = \zeta_0^{-1}(k)$ ([Cv] p.13) and the zeros of $\zeta^{-1}(k)$ are a good approximation to the zeros of the Gutzwiller Semi-Classical Zeta function as shown in section 9. The infinite product in $\zeta^{-1}(k)$ is expressed in (multplied out) a series expansion consisting of fundamental terms (primeorbits) & curvature corrections (pseudocycles, products of primes), ([Cv96] p.138).

$$\zeta^{-1}(k) = 1 - \sum_n f_n \cdot z^n - \sum_n c_n \cdot z^n \tag{8}$$

To improve (or speedup) convergence the series expansion is rearanged so each fundamental term has a shadowing term consisting of associated pseudocyles ([Cv96] p.138) see (10)

$$t_p - (t_{p_1 p_2} + ... + t_{p_1 \cdots p_k})$$

with $p = p_1 ... p_k$

3.4 Factorised zeta functions

The C_{4v}symmetry of the 4-disk (figure 3: having the irreducible representations A_1, A_2, B_1, B_2, E) factorises the Gutzwiller Semi-Classical Zeta function & the dynamical zeta function into a product of the zeta functions of each subspace: ([Cv96] p.295)

$$Z_{qm} = Z_{qm,A_1} Z_{qm,A_2} Z_{qm,B_1} Z_{qm,B_2} Z^2_{qm,E} \ , \ \zeta^{-1} = \zeta^{-1}_{A_1}\zeta^{-1}_{A_2}\zeta^{-1}_{B_1}\zeta^{-1}_{B_2}\zeta^{-2}_{E} \tag{9}$$

The fullysymmetric zeta functions Z_{qm,A_1} & $\zeta^{-1}_{A_1}$ of the A_1 subspace in the fundamental domain contains the leading eigenvalue. The cycle expansion of the A_1 dynamical zeta function is shown here using the 4-disk reduced symbolic dynamics, grouped in terms of same symbolic length ([Cv96] p.294):

$$\begin{aligned}\zeta^{-1}_{A_1}(k) = \ & 1 - [t_0 + t_1 + t_2] - [(t_{10} - t_1 t_0) + (t_{20} - t_2 t_0) + (t_{21} - t_2 t_1)] \\ & - [(t_{100} - t_{10} t_1) + (t_{101} - t_{10} t_1) + (t_{102} - t_{10} t_2 + t_1 t_0 t_2) + (t_{200} - t_{20} t_0) + \\ & (t_{201} - t_{20} t_1 + t_2 t_0 t_1) + (t_{202} - t_{20} t_2) + (t_{211} - t_{21} t_1) + (t_{212} - t_{21} t_2)] \\ & + \cdots\end{aligned} \tag{10}$$

where the $t_{p_1 \cdots p_k}$ are calculated in the fundamental domain (t_2 being the only boundary orbit of the 4-disk system).

4 Cycle Expansion

Having discussed the dynamics of the 4-disk system and the Gutzwiller Semi-Classical Zeta function the following presents how to perform the numerical cycle expansions. The cycle expansion of the Gutzwiller Semi-Classical Zeta function is done by calculating the trace and converting this into the zeta function.

4.1 Calculation of Trace

Constructing the Gutzwiller trace a nonphysical variable z is intoduced to expand the trace, in increasing topological cycle length: n_p. (the original trace is obtained by setting $z = 1$) Numerically a finite truncation up to the order $s \leq N$ of $trG(k)$ is calculated:

$$trG_{(N)}(k) = \sum_s^N C_s(k)\, z^s, C_s(k) = \sum_p n_p \sum_{r=1}^{n_p \cdot r \leq N} \frac{e^{-ir\left(L_p k - \pi \frac{m_p}{2}\right)}}{\left|\Lambda_p^r\right|^{\frac{1}{2}} \left(1 - \frac{1}{\Lambda_p^r}\right)} \delta_{s,n_p r} \tag{11}$$

and the coefficients $C_s(k)$ are calculated from the orbit data by summing up the trace recursively

$$tr_{(N)}G(k)_{(p)} = tr_{(N)}G(k)_{(p-1)} + n_{(p)} \sum_{r=1}^{n_{(p)} \cdot r \leq N} \frac{e^{-ir\left(L_{(p)} k - \pi \frac{m_{(p)}}{2}\right)}}{\left|\Lambda_{(p)}^r\right|^{\frac{1}{2}} \left(1 - \frac{1}{\Lambda_{(p)}^r}\right)} z^{n_{(p)} \cdot r} \tag{12}$$

letting p run through the prime orbits up to topological cycle length $n_{(p)} = N$. ([Cv96] p.140)

4.2 Calculation of zeta functions

The numerical approximation to the Gutzwiller Semi-Classical Zeta function function is expressed in a series expansion in z of the form:

$$Z_{qm}(k) = 1 - \sum_{s} c_s(k)\, z^s\, , Z_{qm(N)}(k) = 1 - \sum_{s}^{N} c_s(k)\, z^s \tag{13}$$

Construction of the zeta function is done from the series expansion of the trace by using the formal relation ([Cv96] p.120) and equating coefficients of (11) & (13) :

$$\begin{gathered} trG_{(N)}(k) = -z\tfrac{\partial}{\partial z}\log Z_{qm}(k) = -z\frac{\frac{\partial}{\partial z}Z_{qm}(k)}{Z_{qm}(k)} \Leftrightarrow \\ trG_{(N)}(k) Z_{qm}(k) = -z\tfrac{\partial}{\partial z}Z_{qm}(k) \\ (C_1 z + C_2 z^2 + \ldots)\cdot(1 - c_1 z - c_1 z^2) = c_1 z + 2c_2 z^2 + 3c_3 z^3 \ldots \end{gathered}$$

giving:

$$c_s(k) = \frac{1}{s}\left(C_s(k) - C_{s-1}(k)c_1(k) - \ldots - C_1(k)c_{s-1}(k)\right) \tag{14}$$

The coefficients of the dynamical zeta function is found by termvise multiplication with the factors: $(1 - t_p)$, for each prime orbit:

$$\zeta^{-1}_{(N)}(k)_{(p)} = \zeta^{-1}_{(N)}(k)_{(p-1)} \cdot \left(1 - t_{(p)}\right), \, t_p = \frac{e^{-i\left(L_p k - \pi\frac{m_p}{2}\right)}}{|\Lambda_p|^{\frac{1}{2}}}\, z^{n_{(p)}} \tag{15}$$

discarding terms z^i of $i \geq N$ ([Cv96] p.141) from which the numerical approximation to the dynamical zeta function is found:

$$\zeta^{-1}_{(N)}(k) = 1 - \sum_{s}^{N} c_s(k)\, z^s \tag{16}$$

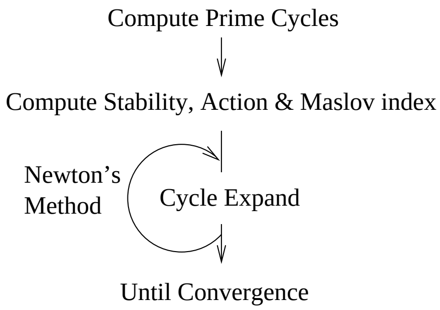

Figure 5: The general algorithm when doing Quantum Chaos by cycle expansion is to find the symbolic dynamics, the prime orbits and compute the cycle data of the "Classical" system (section 6 & section 7). Then the quantum zeta functions are calculated by cycle expansion (section 4.1 & section 4.2) & the zeros are located by Newtons method (section 5) in an intelligent search of the complex plane.

5 Zeros of the zeta functions

The resonances or equivalently the zeros of the Gutzwiller Semi-Classical Zeta function & the dynamical zeta function is found using Newton's method ([Cv96] p.146):

$$k_{n+1} = k_n - \frac{Z_{qm(N)}(k_n)}{\frac{\partial}{\partial k} Z_{qm(N)}(k_n)} \; , \; k_{n+1} = k_n - \frac{\zeta^{-1}_{(N)}(k_n)}{\frac{\partial}{\partial k}\zeta^{-1}_{(N)}(k_n)} \tag{17}$$

The derivative of $Z_{qm(N)}(k)$ becomes:

$$\frac{\partial Z_{qm(N)}(k)}{\partial k} = -\sum_{s}^{N} \frac{\partial}{\partial k} c_s(k) \cdot z^s$$

$$\frac{\partial}{\partial k} c_s(k) = \frac{1}{s}\left\{ \frac{\partial}{\partial k} C_s(k) - \left(\frac{\partial}{\partial k} C_{s-1}(k) \cdot c_1(k) + C_{s-1}(k) \cdot \frac{\partial}{\partial k} c_1(k) \right) - \ldots \right\}$$

where $\frac{\partial}{\partial k} C_s(k)$ is obtained from:

$$\frac{\partial}{\partial k} C_s(k) = \sum_p n_p \sum_{r=1}^{\infty} \frac{-irL_p e^{-ir\left(L_p k - \pi \frac{m_p}{2}\right)}}{\left|\Lambda_p^r\right|^{\frac{1}{2}} \left(1 - \frac{1}{\Lambda_p^r}\right)} \delta_{s, n_p r} \tag{18}$$

calculating this trace similar as (12).

The derivative of the dynamical zeta function is

$$\frac{\partial}{\partial k} \zeta^{-1}(k) = \sum_{p \in P} -v_p t_p z^{n_p} \cdot \prod_{q \in P \setminus p} \left(1 - t_q z^{n_q}\right) \tag{19}$$

which reduces to ([Cv96] p.147)

$$\begin{aligned} \tfrac{\partial}{\partial k}\zeta^{-1}(k) &= -\textstyle\sum_p v_{p_1 \cdot\cdot p_k} t_{p_1 \cdot\cdot p_k} \cdot z^n \\ v_{p_1 \cdots p_k} &= v_{p_1} + \ldots + v_{p_k} = -i\left(L_{p_1} + \ldots + L_{p_k}\right) \end{aligned} \tag{20}$$

Numerically (19) (for small N) is used calculating up to a given order N:

$$\frac{\partial}{\partial k} \zeta^{-1}_{(N)}(k) = \sum_{p \in P}^{n_p \le N} -v_p t_p z^{n_p} \cdot \prod_{q \in P \setminus p}^{n_p \cdot M \le N} \left(1 - t_q z^{n_q}\right) \tag{21}$$

Each time multiplying the last factor out and discarding terms z^i of order $i \ge M$, as shown in the following example: N=2

$\zeta^{-1}(k)$	$(1-t_0)(1-t_1)(1-t_2)(1-t_{10})(1-t_{20})(1-t_{21})$	$1 - t_0 - t_1 - t_2 - t_{10} + t_1 t_0 - t_{20}$ $+ t_2 t_0 - t_{21} + t_2 t_1$
$\frac{\partial}{\partial k}\zeta^{-1}(k)$	$-v_0 t_0 (1 - t_1 - t_2) +$ $-v_1 t_1 (1 - t_0 - t_2) +$ $-v_2 t_2 (1 - t_0 - t_1) +$ $-v_{10} t_{10} - v_{20} t_{20} - v_{21} t_{21}$	$-v_0 t_0 - v_1 t_1 - v_2 t_2 - v_{10} t_{10}$ $(v_2 + v_0) t_1 t_0 - v_{20} t_{20} + (v_2 + v_0) t_2 t_0$ $-v_{21} t_{21} + (v_2 + v_1) t_2 t_1$

For large N a small program doing the direct cycle expansion (20) is used.

The convergence using Newtons method (17) to locate the zeros is illustrated in the following table and on figure 6.

n	$k_n \in Z_{qm}(k_n) = 0$	$k_n \in \zeta^{-1}(k_n) = 0$
1	0.60000000+i0.20000000	0.60000000+i0.20000000
2	0.59129505+i0.15366649	0.59449712+i0.15027495
3	0.59894112+i0.10363602	0.60311850+i0.10133161
4	0.61682036+i0.08079037	0.61953957+i0.08078956
5	0.62322637+i0.07936682	0.62417787+i0.07993107
6	0.62370093+i0.07963831	0.62424184+i0.08004193
7	0.62371782+i0.07967248	0.62424175+i0.08004190
8	0.62371740+i0.07967516	0.62424175+i0.08004190
9	0.62371727+i0.07967530	0.62424175+i0.08004190

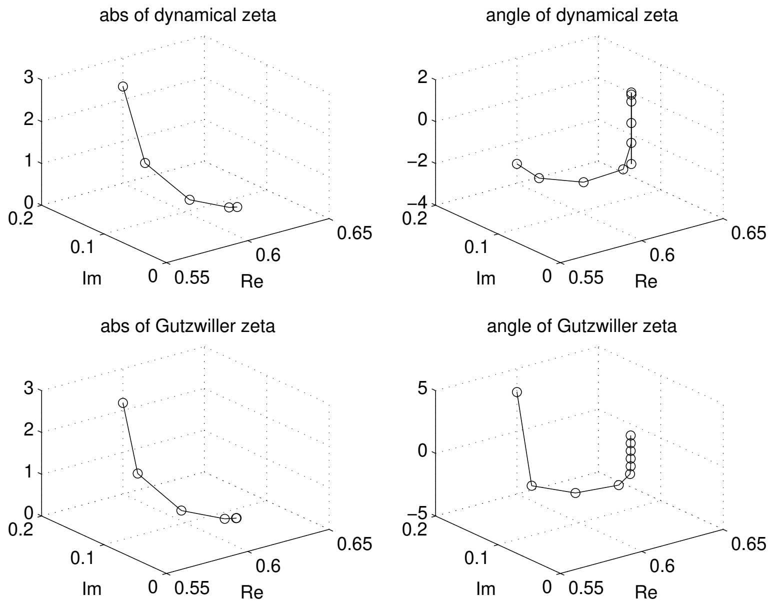

Figure 6: Top left & right: Convergence of the absolute value (left) & the corresponding angle (right) of $\zeta^{-1}(k)$. Bottom left & right: Convergence of the absolute value (left) & the corresponding angle (right) of $Z_{qm}(k)$.

The following sections describe how to calculated the quantities used in the above.

6 Periodic Cycles

Given a specific itinerary the (mapping into the) corresponding periodic cycle in the 4-disk pinball is found by path length minimization: ([Cv96] p.106)

- To each letter in the specific itinerary an arbitrary point on the corresponding disk is specified, resulting in an initially non-minimal cycle.
- The length of this cycle is minimized by varying the points on the disk $\to$ physical cycle.

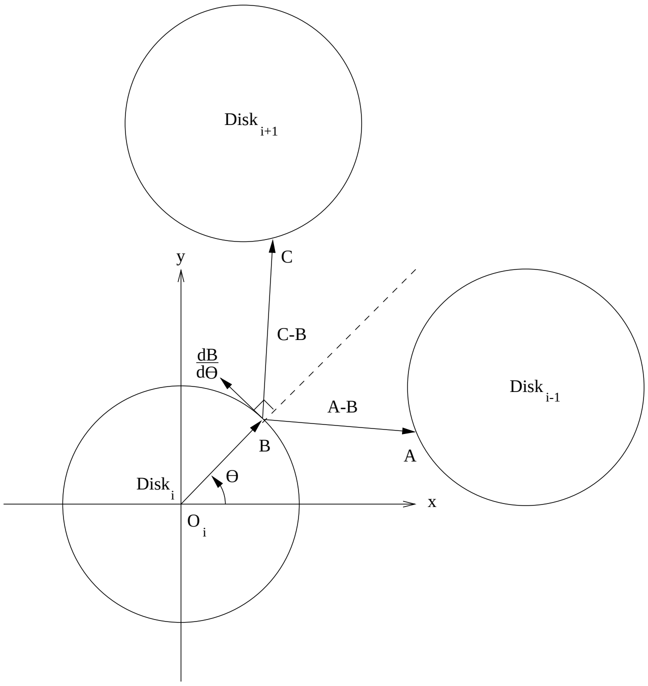

Figure 7: Illustration of the used vectors and angles when minimizing the cycle length.

The minimization is done iteratively improving each disk point using Newton's method. Minimizing the path length L_p of the orbit $\leftrightarrow$ minimization of each segment $L_i \forall i$,varying point P_i. Let $A = O_iP_{i-1}$ (constant), $B = O_iP_i$,$C = O_iP_{i+1}$ (constant). (figure 7)

$$\begin{aligned} L_i &= |A - B| + |C - B| \\ &= \sqrt{A^2 + B^2 - 2A \cdot B} + \sqrt{C^2 + B^2 - 2C \cdot B} \end{aligned} \tag{22}$$

with B fixed on the i'th disk: B(θ)=a(cos(θ),sin(θ)). The minima is found at:

$$\min(L_i(\theta)) \Rightarrow \frac{dL_i(\theta)}{d\theta} = 0 \tag{23}$$

(verifying it is the minima and not the maxima)

$$f_i(\theta) = \frac{dL_i(\theta)}{d\theta} = -\left[A\left(A^2 + B^2 - 2A \cdot B\right)^{-\frac{1}{2}} + C\left(C^2 + B^2 - 2C \cdot B\right)^{-\frac{1}{2}}\right] \cdot \frac{dB(\theta)}{d\theta} \tag{24}$$

where $\frac{dB(\theta)}{d\theta} = a(-\sin(\theta), \cos(\theta))$
The zero of (24) is found using Newton's method:

$$\theta_{n+1} = \theta_n - \frac{f_i(\theta)}{\frac{d}{d\theta} f_i(\theta)} \tag{25}$$

where 1'sth derivative of $f_i(\theta)$ used in (25) becomes:

$$\frac{df_i(\theta)}{d\theta} = F - (AD^{-\frac{1}{2}} + CE^{-\frac{1}{2}}) \cdot B$$

setting D=$A^2 + a^2 - 2A \cdot B$, E=$C^2 + a^2 - 2C \cdot B$, F=$\left(A^2 D^{-\frac{3}{2}} + C^2 E^{-\frac{3}{2}}\right) a^2$
The convergence is improved by iterating L_i in parallel:

$$\underline{\theta}_{n+1} = \underline{\theta}_n - \underline{F}(\underline{\theta}_n)$$

with $\theta_{i,n}$ redefined to be the current angle of the point on disk i, in iteration n.

$$\begin{bmatrix} \theta_1 \\ \theta_2 \\ \vdots \\ \theta_{m-1} \\ \theta_m \end{bmatrix}_{n+1} = \begin{bmatrix} \theta_1 \\ \theta_2 \\ \vdots \\ \theta_{m-1} \\ \theta_m \end{bmatrix}_n - \begin{bmatrix} \frac{f_1(\theta_{1,n})}{\frac{d}{d\theta} f_1(\theta_{1,n})} \\ \frac{f_2(\theta_{2,n})}{\frac{d}{d\theta} f_2(\theta_{2,n})} \\ \vdots \\ \frac{f_{m-1}(\theta_{m-1,n})}{\frac{d}{d\theta} f_{m-1}(\theta_{m-1,n})} \\ \frac{f_m(\theta_{m,n})}{\frac{d}{d\theta} f_m(\theta_{m,n})} \end{bmatrix} \tag{26}$$

Numerical convergence is further improved by using the updated data at each iteration: $\frac{f_i(\theta_{i,n})}{\frac{d}{d\theta} f_i(\theta_{i,n})}$ uses the new point calculated by minimizing the previous $\theta_{i-1,n+1}$ in (26).

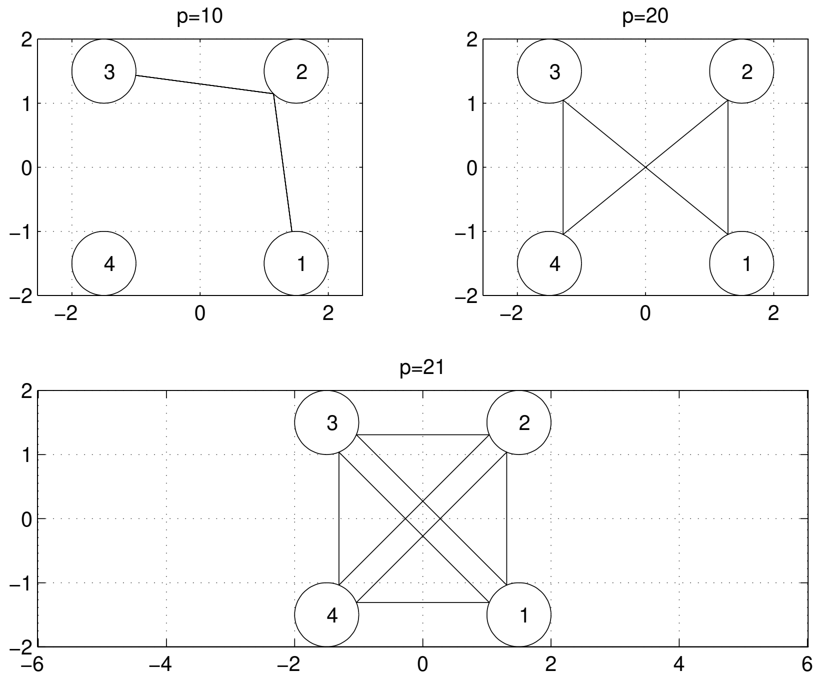

Figure 8: Illustration of the length 2 prime cycles (in the reduced symbolic dynamics): 10,20,21 and their corresponding orbits in the full domain (R=3:a).

7 Stability

The stability of the periodic orbits are evalutated from the eigenvalues of the jacobian along the flow.

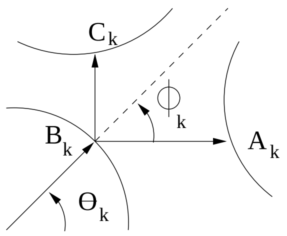

Figure 9: Illustrating the incomming angle ϕ_k and the vectors used.

The jacobian is calculated from ([Cv96] p.80) & consists of a free flight jacobian J$_{sf}$ & a reflection jacobian:J$_{sr}$:

$$\underline{\underline{J}}_{sf} = \begin{bmatrix} 1 & \tau_k \\ 0 & 1 \end{bmatrix}, \underline{\underline{J}}_{sr} = \begin{bmatrix} -1 & \\ \frac{2}{\rho_k \cos(\phi_k)} & -1 \end{bmatrix} \tag{27}$$

τ_k being the flight time from bounce k-1 to k (equal to the length between the disks since the velocity is set =1) , ϕ_k is the incident angle from the normal to the disk surface (figure 9) & ρ_k is the curvature of the disk. The curvature of a disk with radius 1 is: $\rho_k = -1$

The total jacobian of a periodic orbit with lenght n$_p$ is a product of J$_{sf}$,J$_{sr}$ along the orbit:

$\underline{\underline{J}} = (-1)^{n_p} \prod_{k=1}^{n_p} \begin{bmatrix} 1 & \tau_k \\ 0 & 1 \end{bmatrix} \begin{bmatrix} 1 & \\ \frac{2}{\cos(\phi_k)} & 1 \end{bmatrix} = (-1)^{n_p} \prod_{k=1}^{n_p} \begin{bmatrix} 1 + \frac{2\tau_k}{\cos(\phi_k)} & \tau_k \\ \frac{2}{\cos(\phi_k)} & 1 \end{bmatrix}$

$\tau_k = |A_k - B_k|, \cos(\phi_k) = \frac{B_k \cdot (A_k - B_k)}{|B_k||A_k - B_k|}$ inserted gives:

$$\underline{\underline{J}} = (-1)^{n_p} \prod_{k=1}^{n_p} \begin{bmatrix} 1 + \frac{2|B_k||A_k - B_k|^2}{B_k \cdot (A_k - B_k)} & |A_k - B_k| \\ \frac{2|B_k||A_k - B_k|}{B_k \cdot (A_k - B_k)} & 1 \end{bmatrix} \tag{28}$$

The stability Λ_p used in calculating the zeta functions (4),(5) & (10) is the product of the expanding eigenvalues, in 2-d there are two eigenvalues therefore Λ_p = max eigenvalues($\underline{\underline{J}}$) wich for 2-d matrices becomes :

$$\Lambda_p = \frac{1}{2} tr \underline{\underline{J}} + \frac{1}{2}\sqrt{(tr\underline{\underline{J}})^2 - 4} \tag{29}$$

8 Quantum Mechanics

The quantum mechanical resonances of the 4-disk problem are obtained by the zeros of the following matrix ([Wi] p.3) & ([Wi] p.6):

$$M_{mm'} = \sum_{j,j'} M_{mm'}^{JJ'}$$

$$M_{mm'}^{JJ'} = \delta^{JJ'}\delta_{mm'} + (1 - \delta^{JJ'}) \left(\frac{a_j}{a_{j'}}\right) \frac{J_m(ka_j)}{H_{m'}^{(1)}(ka_j)} H_{m-m'}^{(1)}(kR_{jj'}) e^{i(m\alpha_{j'j} - m'\alpha_{jj'})}(-1)^m$$

where :$R_{jj'}$ disk j to j' center distance, $a_j = 1$, $\alpha_{j'j}$ angle from disk j to j' measure in the local coordinate system of j.

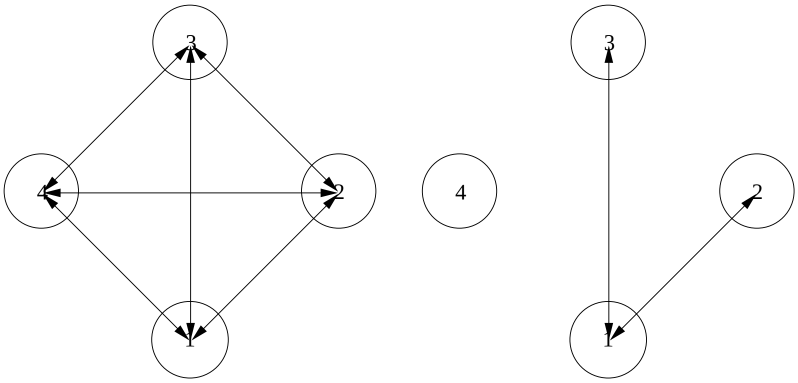

Figure 10: The C_{4v} symmetry of the systems reduces $M_{mm'}$ to the sum of the (J, J') pairs in the fundamental domain.

In the four disk case the C_{4v} symmetry of the system and therefore the symmetry in the pairs (J, J'), (see figure 10) reduces M to:

$$M_{mm'} = 4M^{1,1}_{mm'} + 4\left(M^{1,2}_{mm'} + M^{2,1}_{mm'}\right) + 2\left(M^{1,3}_{mm'} + M^{3,1}_{mm'}\right)$$

with $\alpha_{12} = \frac{3\pi}{4}, \alpha_{21} = \frac{\pi}{4}, \alpha_{13} = \frac{\pi}{2}, \alpha_{31} = \frac{\pi}{2}$, & $R_{12} = R, R_{13} = \sqrt{2}R$ the matrix becomes:

$$\begin{aligned} M_{mm'} &= \delta_{mm'} + \frac{J_m(k)}{H^{(1)}_{m'}(k)} H^{(1)}_{m-m'}(kR)\left(e^{i\frac{3\pi}{4}(m+m')} + e^{i\frac{\pi}{4}(m+m')}\right) \\ &\quad + \frac{J_m(k)}{H^{(1)}_{m'}(k)} H^{(1)}_{m-m'}(k\sqrt{2}R) e^{i\frac{\pi}{2}(m+m')} \end{aligned} \tag{30}$$

Since $\underline{\underline{M}}$ is of the form $\underline{\underline{M}} = \underline{\underline{A}} + \underline{\underline{1}}$, the determinant is expanded in the trace:

$$\det(\underline{\underline{M}}(k)) = 1 + trA + \frac{1}{2}((trA)^2 - trA^2) + \ldots$$

where the series and $\underline{\underline{A}}$ is truncated in numerical calculations:

$$trA_{(N)} = \sum_{n}^{N} A_{n,n} \tag{31}$$

From $\det(\underline{\underline{M}}(k)) = 1 + trA_{(5)}$, the one of the lowest resonances is found to be 0.589-0.026i (see the following section 9).

9 Results

The A_1 resonances of the 4-disk pinball calculated through cycle expansion is illustrated on figures 11, 12 & 13 and the 7 lowest resonances (ordered after $Real(k_i) < Real(k_{i+1})$) are shown in the following table, together with a few quantum mechanical resonances, and the relative error in the real part.

n	Gutzwiller SC Zeta function (N=8)	quantum mechanics	$rel.error_{real\ part}$
1	0.00000000+i0.18939480		
2	0.62258725+i0.08447474	0.589-i0.026	0.056
3	0.98435585+i0.17763583		
4	1.92204284+i0.18130125		
5	2.30999030+i0.08895497	2.27-i0.08	0.018
6	2.90348054+i0.18522368		
7	3.48689086+i0.10337329	3.42-i0.09	0.017

As the table shows there is a weak correspondence between the cycle expansion and the exact data for the lowest resonances, the relative error being $\approx 6\%$ in the real part of the spectra. This is expected as the semi-classical cycle expansion is inaccurate in the quantum limit, where higher $\hbar$-corrections are required ([Wi] p.5). The correctness of the cycle expansion improves when moving up in resonances and at the seven'th resonnance the relative error has reduced to 0.017 in the real part. The cycle expansion is expected to approximate the quantum spectrum with much higher accuracy at higher resonances (view the plots of Cvitanović ([Cv] p.15)). (The calculation of the quantum mechanical data has here only been done for a few low resonances. The reverse imaginary sign of the cycle data comes from the negative sign of in the exponent of t_p in (4) & (5) as compared to ([Wi] p.2) therefore since the spectrum is symmetric in the real part: $e^{i(a+ib)} = e^{-b+ai}$, $a = -a$, $\rightarrow e^{-b-ai} = e^{-i(a-ib)}$.)

The resonance spectra (figure 12) has a mean spacing of 0.79 and is approximately given by $\frac{2\pi}{\overline{L}}$, where $\overline{L}$ is average cycle lengths of the t_0 , t_1 & t_2 cycles.

$$\overline{L} = \tfrac{1}{3}(L_0 + L_1 + L_2) = 7.19, \quad \tfrac{2\pi}{\overline{L}} = 0.875 \tag{32}$$

The spectra of (figures 11 & 13, order N=4) are to diffuse to display any detailed structure (only wage lines are visible). For the cycle data with order N=8 (figure 12) some zeros gets canceled/moved by the higher calculation order and more structure is revealed (a beginning beating pattern is formed), but not as clearly as in ([Cv] p.15). However all plots show some resemblence to the 3-disk spectra.

A larger zero-scan (but with lower resolution) of the zeta functions (N=4) is illustrated on figures 15 & 16 .

The convergence of the Gutzwiller Semi-Classical Zeta function & the dynamical zeta function as a function of the order N=$max(n_p)$ is shown in the following table for the resonance k=.6225+i0.0844:

$\max(n_p)$	Cycles	$k_n \in Z_{qm}(k_n) = 0$	$k_n \in \zeta^{-1}(k_n) = 0$
1	3	0.62262174+i0.16954434	0.60605031+i0.17076442
2	6	0.65240678+i0.08835077	0.65136752+i0.09330596
3	14	0.63162450+i0.07835444	0.63212117+i0.07980286
4	32	0.62371725+i0.07967530	0.62424175+i0.08004190
5	80	0.62134814+i0.08238501	0.62165412+i0.08234224
6	196	0.62150428+i0.08414607	0.62158568+i0.08401646
7	508	0.62222143+i0.08461216	0.62219510+i0.08454540
8	1318	0.62258725+i0.08447474	0.62255640+i0.08446633

Showing the Gutzwiller Semi-Classical Zeta function & the dynamical zeta function converges with the same order of magnetude. This is also demonstrated on figure 14 showing the logarithm of the absolute values of the coefficients in the series expansion (33) of the Gutzwiller Semi-Classical Zeta function & the dynamical zeta function (around the same resonance) llustrating an exponetial decay.

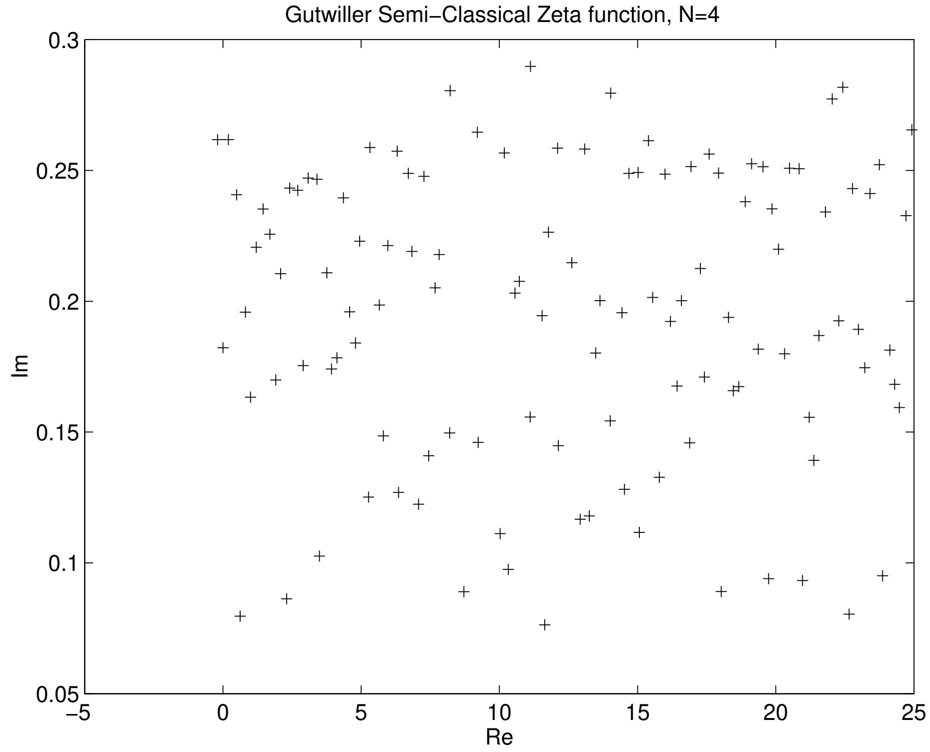

Figure 11: Illustrating the resonances of $Z_{A_1,qm}(k)$ in the complex plane. Calculated for N=4 (32 cycles).

$$Z_{qm}(k) = 1 - \sum_s c(k) \cdot z^s, \zeta^{-1}(k) = 1 - \sum_s t_s \cdot z^s \tag{33}$$

Finally a beautyfull surface & countour plot of the Gutzwiller Semi-Classical Zeta function (N=4) are shown on figures 17, 18.

10 Conclusion

The calculated resonances are in resonable agrement with the resonances calculated by quantum mechanics. Further more the convergence properties of the Gutzwiller Semi-Classical Zeta function and the dynamical zeta function have been illustrated.

References

[Cv96] Cvitanović, Predrag, Classical and Quantum Chaos: A Cyclist Treatise. preliminary version may 22,1996.

[Cv] Cvitanović Predrag, etc. : Quantum Fluids and Classical Determinants

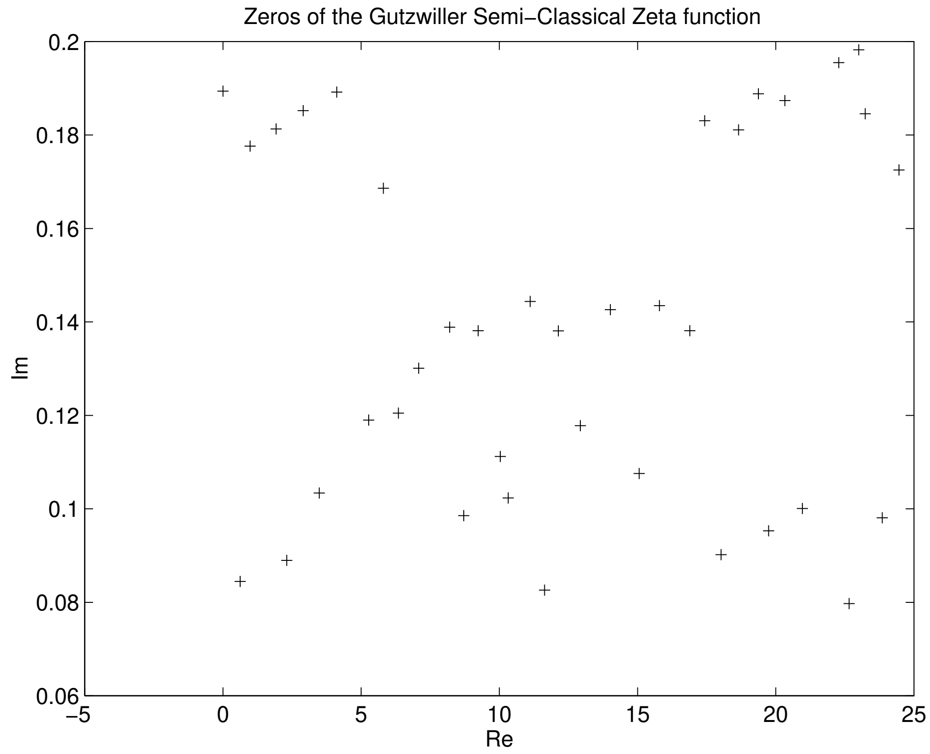

Figure 12: Illustrating the resonances of $Z_{A_1,qm}(k)$ in the complex plane. Calculated for N=8 (1318 cycles).

[Wi] Wirsba, Andreas & Henseler, Michael: The missing link between the quantum-mechanical and semiclassical dertermination of scattering poles.

A Cycle data

The following is a list of the (first 20) cycle data used in calculating the Gutzwiller Semi-Classical Zeta function & the dynamical zeta function.

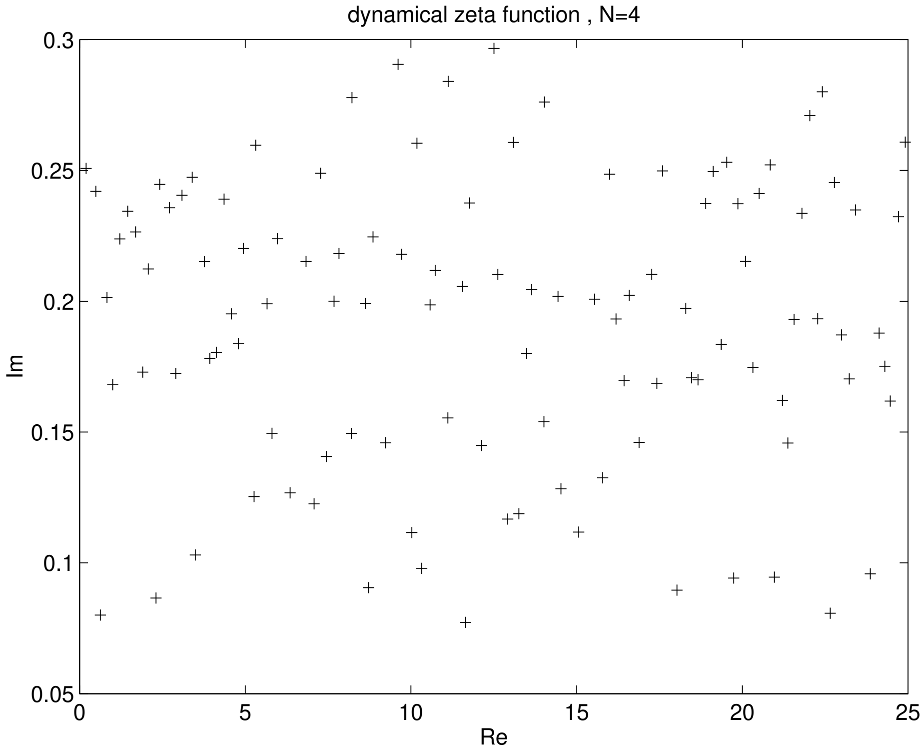

Figure 13: Illustrating the resonances of $\zeta_{A_1}^{-1}(k)$ in the complex plane. Calculated for N=4 (32 cycles).

p	n_p	Λ_p	L_p	m_p
1	1	9.89897949	4.000	2
2	1	14.90346425	4.586	2
3	1	222.11324680	12.971	4
4	2	172.00700895	8.680	4
5	2	186.33506239	10.829	4
6	2	177.86631203	10.790	4
7	3	1741.52976179	12.690	6
8	3	1924.81205439	14.862	6
9	3	2516.35438402	13.260	6
10	3	1813.16958709	14.816	6
11	3	-2776.30493665	15.397	6
12	3	2870.59276699	15.430	6
13	3	2707.65278494	17.293	6
14	3	2719.64694592	17.296	6
15	4	17287.64374225	16.691	8
16	4	19168.03817384	18.865	8
17	4	30801.60842767	19.486	8
18	4	42611.58133250	20.015	8
19	4	33178.59340362	21.619	8
20	4	25357.34710220	17.269	8

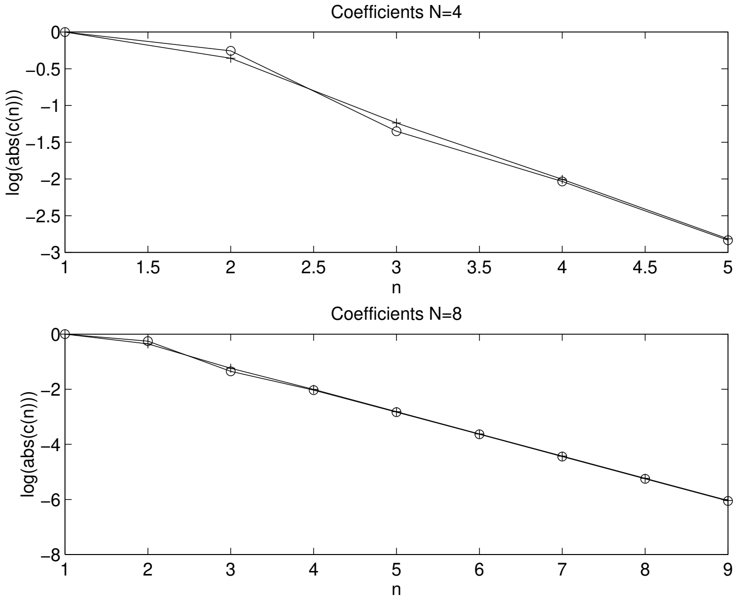

Figure 14: The logaritm of the absolute value of the coefficients ($\circ = Z_{qm}(k)$,$+ = \zeta^{-1}(k)$) around k=.6225+i0.0844. Top for N=4. Bottom for N=8.

B Programs

The following presents the programs used in the calculations:

- C-program: Prime1 is a C program calculating the itineries of the primeorbits in the fundamental domain.
- Matlab-programs: Only some of the important programs are listed here. Several others exist to make different plots & calculations mainly used by these programs:
  1. playf4d: Calculating the cycle data.
  2. pinball: Calculates a pinball trajectory.
  3. gfred: Calculates Gutzwiller Semi-Classical Zeta function using tr2zeta & gtrace
  4. gzeta: Calculates the dynamical zeta function
  5. dgzeta: Calculates the derivative of the dynamical zeta function
  6. plotg2: Calculates surface plots & contours
  7. resonz4-8: Calculates the resonanses of the dynamical zeta function of 4 and 8 order respectively.
  8. resonf4-8: Calculates the resonanses of Gutzwiller Semi-Classical Zeta function of 4 and 8 order respectively.
- Matematica-program: q4exact calculates som exact quantum resonances

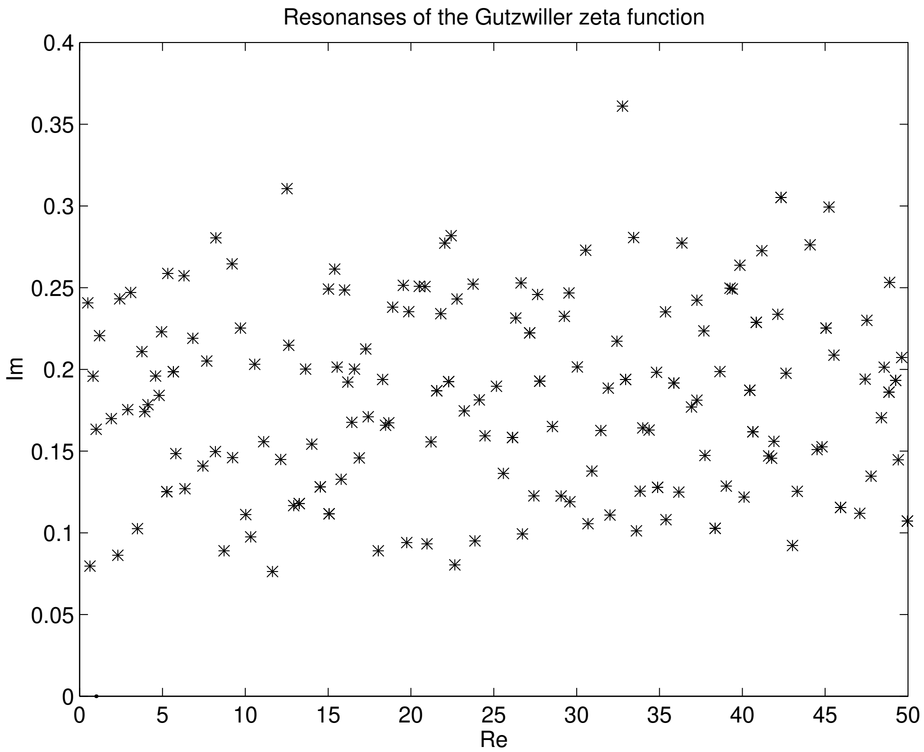

Figure 15: Illustrating the resonances of $Z_{A_1,qm}(k)$ in the complex plane. Calculated for N=4 (32 cycles).

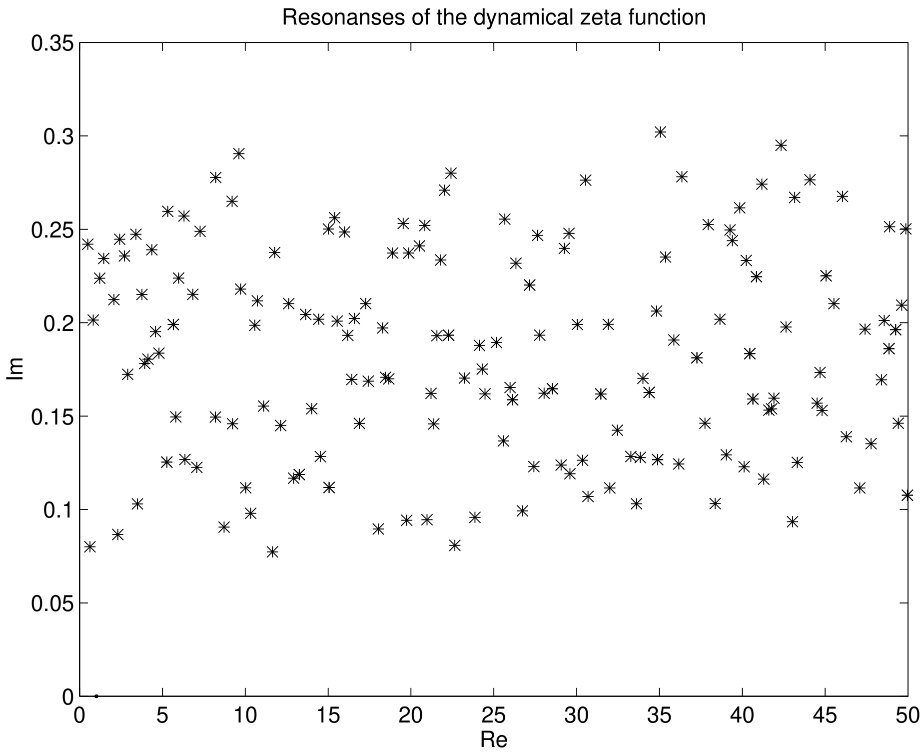

Figure 16: Illustrating the resonances of $\zeta_{A_1}^{-1}(k)$ in the complex plane. Calculated for N=4 (32 cycles).

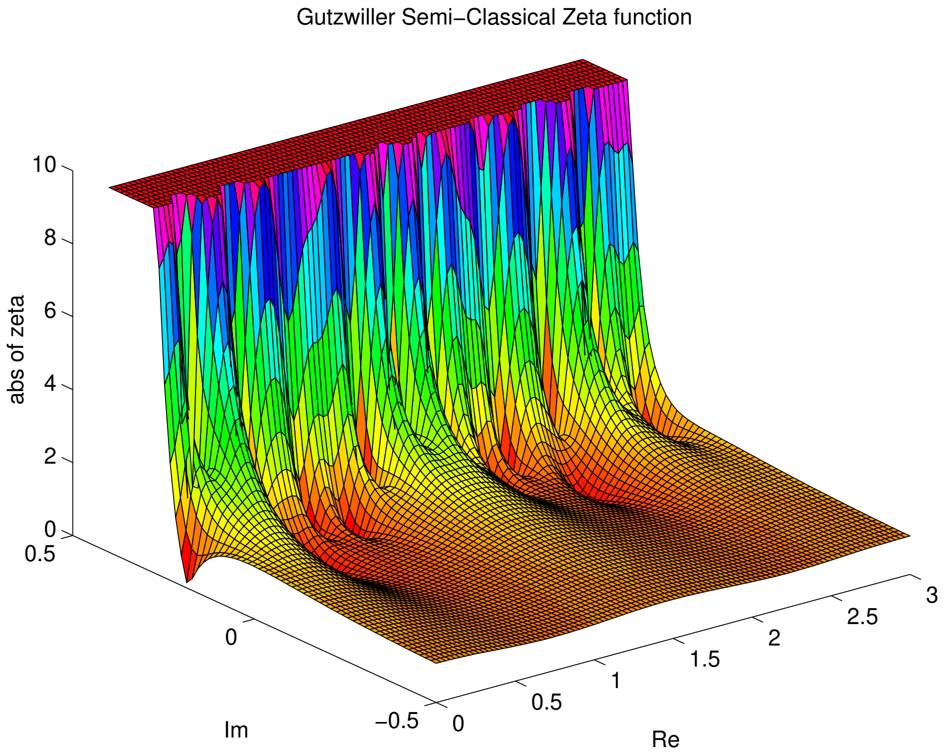

Figure 17: 3-D surface plot of the Gutzwiller Semi-Classical Zeta function (N=4) (the absolute value is limited to maximum 10 in the plot). The resonances lie in the deep wallies of the "landscape".

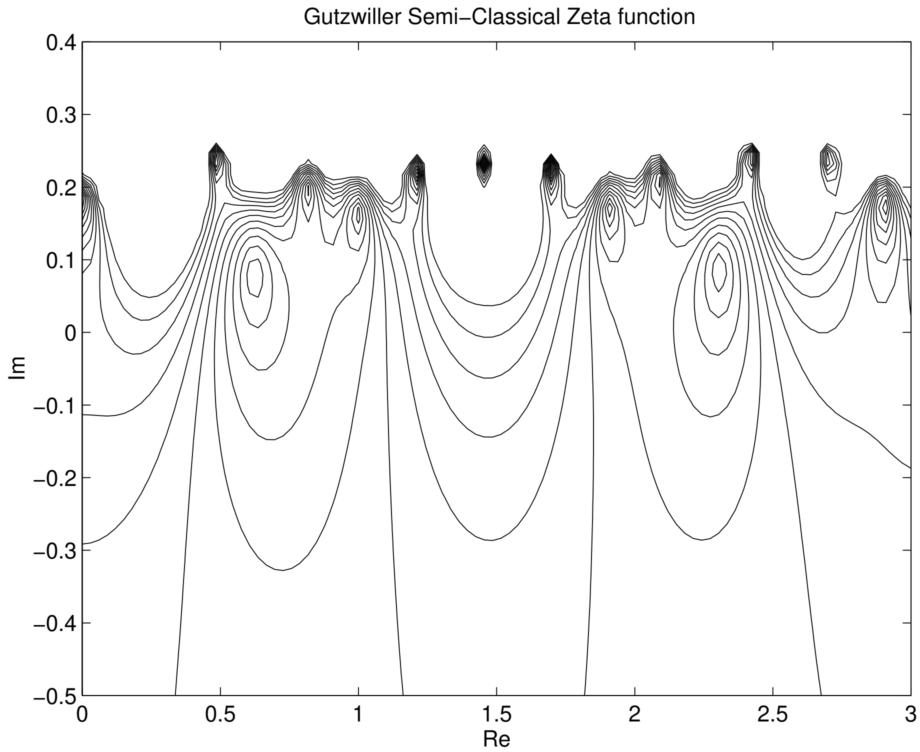

Figure 18: Contour plot of the Gutzwiller Semi-Classical Zeta function (N=4). Showing the resonances incircled by contour lines.